Molecular Packing and Solid-State Fluorescence of Alkoxy-Cyano Substituted Diphenylbutadienes: Structure of the Luminescent Aggregates

Riju Davis,[†] N. S. Saleesh Kumar,[†] Shibu Abraham,[†] C. H. Suresh,[‡] Nigam P. Rath,[§] Nobuyuki Tamaoki,[||] and Suresh Das*,[†]

Photosciences and Photonics, Chemical Sciences and Technology Division, National Institute for Interdisciplinary Science and Technology (Formerly Regional Research Laboratory), CSIR, Trivandrum - 695 019, Kerala, India, Computational Modeling and Simulation Section, National Institute for Interdisciplinary Science and Technology, CSIR, Trivandrum - 695 019, Kerala, India, Department of Chemistry and Biochemistry and Center for Nanoscience, University of Missouri-St. Louis, Missouri 63121, and Molecular Smart System Group, Nanotechnology Research Institute, National Institute of Advanced Industrial Science and Technology (AIST), 1-1-1, Higashi, Tsukuba, Ibaraki-305-8565, Japan

Received: October 26, 2007

A detailed study on the photophysical properties of a series of alkoxy substituted diphenylbutadienes in solution and in the solid state providing a molecular level understanding of the factors controlling their solid-state luminescence behavior is reported. Our studies provide clear evidence for exciton splitting in the solid state resulting in red-shifted emission for this class of materials. The role of the number of alkoxy substituents and the alkyl chain length in controlling the nature of the molecular packing and consequently their fluorescence properties has been elucidated. Whereas in the di- and tri-alkoxy substituted derivatives, the solid-state fluorescence was independent of the length of the alkyl chains, in the monoalkoxy substituted derivatives, increasing the length of the alkyl chain resulted in a visual change in fluorescence from green to blue. On the basis of the analysis of the molecular packing in the single crystals, this difference could be attributed to fluorescence arising from aggregates with an edge-to-face alignment in the molecules possessing short alkyl chains (methyl and butyl) to monomer fluorescence in the long alkyl chain containing derivatives.

Introduction

The past decade has witnessed a spurt of interest in the study of optical and electronic properties of π-conjugated materials[1] stimulated mainly by the potential for their application in devices such as light-emitting diodes,[2] photovoltaic devices,[3] and field effect transistors.[4] Many of these devices, which make use of organic π-conjugated polymers and small molecules as key elements, are rapidly approaching commercialization.[5] An attractive feature of organic materials is the ability to fine-tune their optical and electronic properties by subtle manipulation of their basic molecular structure. In this respect, although structure−property relationships of organic electronic materials are fairly well established at the molecular level, factors that control their bulk properties are still not fully understood.[6] Bulk properties such as luminescence, exciton migration, and carrier mobility depend strongly upon the intermolecular dipole coupling, which are determined by the relative positions of adjacent molecules and directions of their dipole moments.[7,8] Understanding the nature of the interactions that determine the packing of molecules in the solid state and how they affect the optical and electronic properties of the materials is therefore essential for tuning their properties.[9] The absorption spectra of π-conjugated systems are often known to undergo a red-shift in the solid state compared to that in the solution phase, resulting in reduction of luminescence efficiency.[7a,8a] These effects are generally attributed to formation of molecular aggregates. Several recent studies have, however, shown that molecular aggregation can lead to significant enhancement in luminescence efficiency.[10] Various factors such as restricted molecular motion in the aggregates or planarization have been suggested for explaining this phenomenon. Aggregation of molecules can also lead to exciton coupling. In this context, formation of J-type aggregates is of special interest, in view of their propensity to exhibit cooperative and coherent phenomena such as giant oscillator strength and superradiance, which can result in strongly emissive systems.[11] Elucidating root causes of the observed differences in the luminescence spectra and efficiencies in the solid state compared to that observed in solution is, however, complicated by the absence of structural features in the solid-state spectra and difficulties in elucidating the exact nature of the molecular packing.

During the course of our studies on the use of donor−acceptor-substituted diphenylbutadienes for the design of photofunctional materials such as liquid crystals and gels, we have observed that the bulk optical properties of monoalkoxy substituted diphenylbutadienes were highly sensitive to molecular structure and environmental factors such as temperature.[12] The derivatives with longer alkoxy chains (octyloxy, C8, and dodecyloxy, C12) exhibited monomer-like fluorescence ($\lambda_{max} \sim 450$ nm) in the solid state, whereas those of the short alkoxy chain derivatives (methoxy, C1, and butyloxy, C4) were significantly broader and red-shifted ($\lambda_{max} \sim 500$ nm). The C8 derivative in particular was observed to possess two thermally interconvertible polymorphic states with drastically different

* To whom correspondence should be addressed. E-mail: sdaas@rediffmail.com.
[†] Photosciences and Photonics Section: Fax. No. 91-471-2490186.
[‡] Computational Modeling and Simulation Section.
[§] University of Missouri-St. Louis.
[||] Molecular Smart System Group.

10.1021/jp710352m CCC: $40.75
Published on Web 01/23/2008

CHART 1

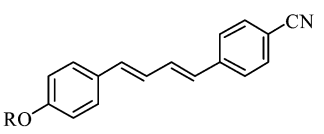

MBC1: R = CH_3 **MBC8**: R = C_8H_{17}

MBC4: R = C_4H_9 **MBC12**: R = $C_{12}H_{25}$

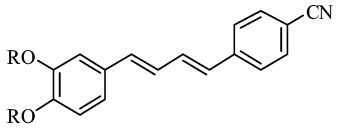

DBC8: R = C_8H_{17} **DBC12**: R = $C_{12}H_{25}$

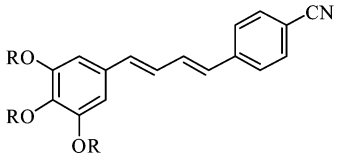

TBC1: R = CH_3 **TBC4**: R = C_4H_9 **TBC12**: R = $C_{12}H_{25}$

fluorescence properties. In the stable crystalline state, it exhibited a monomer-like blue fluorescence ($\lambda_{max} \sim 450$ nm), whereas in its kinetically trapped metastable state formed by cooling its melt, it exhibited strong green fluorescence ($\lambda_{max} \sim 500$ nm), very similar to that observed for the derivatives with short alkoxy chains.

In this paper, we report a detailed study of the absorption and emission properties of some mono-, di-, and tri-alkoxy substituted diphenylbutadienes (Chart 1) in solution and in the solid phase, with special emphasis on the role of crystal packing motifs in determining the bulk optical properties and the structure of the aggregates responsible for the red-shifted aggregate emission.

Experimental Section

Synthesis. The synthesis and characterization of monoalkoxy-cyano substituted diphenylbutadienes have been reported earlier.[13a] The di-alkoxy- and tri-alkoxy-cyano substituted diphenylbutadiene derivatives were synthesized in a similar manner by the Wittig−Horner reaction of the corresponding cinnamaldehyde with the phosphonate ester of *p*-cyanobenzyl bromide using NaH as base in tetrahydrofuran (THF). The compounds were purified by column chromatography using silica gel (100−200 mesh) as the stationary phase and hexane/ethyl acetate mixture (9:1) as the eluent. Further purification (>99%) was carried out using preparative high-performance liquid chromatography (HPLC). The structures of these derivatives were confirmed using IR, NMR, high-resolution mass spectrometry (HRMS), and elemental analysis.[14]

Instrumentation. The purity of the compounds studied was established by HPLC analyses which were carried out using a Shimadzu HPLC system.[13a,14] IR spectra were recorded on a Nicolet Impact, Bomem MB Series 400 D Fourier transform infrared (FT-IR) spectrometer. NMR spectra were measured on Bruker DPX 300 MHz spectrometers. Tetramethylsilane (TMS) was used as the internal standard, and chloroform-d ($CDCl_3$) was used as the solvent. High-resolution mass spectral (HRMS) analysis was obtained from JEOL JMS600 instrument. Elemental analysis was recorded using ThermoFinnigan FLASH EA 1112 CHNS analyzer. Absorption spectra were recorded on a Shimadzu UV-3101PC UV−vis−NIR spectrophotometer. Diffuse reflectance absorption spectra were recorded using a Shimadzu integrating sphere assembly attached to a Shimadzu UV−vis−NIR 3101 PC spectrophotometer. $BaSO_4$ was used as the reflectance standard.

The excitation and emission spectra were recorded on a SPEX Fluorolog F112X spectrofluorimeter. Fluorescence quantum yields, with an estimated reproducibility of around 10%, were determined by comparison with quinine sulfate in 0.1 N H_2SO_4 ($\Phi_f = 0.546$), which was used as the fluorescence standard. The quantum yields of fluorescence of these derivatives in solution were measured using a modified method because of strong photoisomerization of the *EE* isomers of these derivatives into their nonfluorescent *EZ* and *ZE* forms.[13a,b] The decrease in intensity at the fluorescence maximum was monitored as a function of time till the photostationary state was reached. The fluorescence spectrum recorded in the photostationary state was then extrapolated to time $t = 0$.

Measurements of solid-state photoluminescence were carried out using the front face emission scan mode on an SPEX Fluorolog F112X spectrofluorimeter. Solid-state fluorescence quantum efficiency was measured using a calibrated integrating sphere in an SPEX Fluorolog spectrofluorimeter. A Xe-arc lamp was used to excite the thin-film sample placed in the sphere, with 380 nm as the excitation wavelength. Samples were prepared by heating the material placed between two glass coverslips, which was heated above the respective melting points and cooled to room temperature to obtain good films. The quantum yield of solid-state fluorescence was determined by comparing the spectral intensities of the lamp and the sample emission using a reported procedure.[15] Using this experimental setup and the integrating sphere system, the solid-state fluorescence quantum yield of a thin film of the standard green OLED material tris-8-hydroxyquinolinolato aluminum (Alq_3) was determined to be 19% ± 2%, which is consistent with previously reported values.[16] CIE, Commission Internationale de l'Eclairage (International Commission on Illumination), chromaticity coordinates (1931) (x, y) in thin films were calculated using HORIBA Jobin Yvon Color Calculator provided with integrating sphere. Fluorescence lifetimes were measured using IBH (FluoroCube) time-correlated picosecond single photon counting (TCSPC) system. Solutions or thin films were excited with a pulsed diode laser (<100 ps pulse duration) at a wavelength of 375 nm (NanoLED-11) with a repetition rate of 1 MHz. The detection system consisted of a microchannel plate photomultiplier (5000U-09B, Hamamatsu) with a 38.6 ps response time coupled to a monochromator (5000M) and TCSPC electronics (data station Hub including Hub-NL, NanoLED controller, and preinstalled fluorescence measurement and analysis studio (FMAS) software).

Single crystal analyses were carried out in a Bruker SMART-CCD diffractometer, structure determination and refinement was carried out with SAINT (SAINTPLUS Version 6.22, Bruker AXS, Madison, WI) and SHELXTL[17a] software packages, and

TABLE 1: Absorption and Emission Characteristics of Alkoxy Diphenyl Butadienes in Solvents of Varying Polarity[a]

	toluene				acetonitrile			
compound	abs. λ_{max} (nm)	ems. λ_{max} (nm)	Φ_f	τ_f (ns)	abs. λ_{max} (nm)	ems. λ_{max} (nm)	Φ_f	τ_f (ns)
MBC1	363	435	0.02		356	475	0.01	
MBC4	365	435	0.03		358	480	0.01	
MBC8	364	435	0.02		355	477	0.01	
MBC12	364	435	0.03		356	482	0.01	
DBC8	372	435	0.09	0.18	366	504	0.05	0.21
DBC12	367	440	0.09	0.18	366	504	0.05	0.17
TBC1	366	450	0.20	0.35	358	520	0.14	0.34
TBC4	368	456	0.24	0.39	361	522	0.16	0.49
TBC12	368	451	0.24	0.43				

[a] Φ_f, fluorescence quantum yield; τ_f, fluorescence lifetime. In the monoalkoxy series, the lifetime of the excited-state species was within the time resolution of the instrument (<100 ps). The value of fitting parameter (χ^2) lies between 1.0 and 1.2. The quantum yield of **TBC12** in acetonitrile could not be calculated because of poor solubility.

the empirical absorption correction was carried out with the SADABS[17b] program. For crystal structure visualization, Mercury (CSD software)[18] and ChemCraft were used.

Results and Discussion

Photophysical Properties in Solution. The absorption and emission properties of the alkoxybutadiene derivatives in toluene and acetonitrile are summarized in Table 1. The absorption spectra of these derivatives were fairly insensitive to the number and length of the alkoxy substituents and to the solvent polarity. The insensitivity of the absorption spectra of these molecules to solvent polarity is indicative of the dipole moments of their ground and excited states being nearly the same. Their fluorescence spectra, however, exhibited a marked bathochromic shift with increasing solvent polarity, indicating that the dipole moments of their emissive states are significantly higher compared to that of their ground states. These results suggest that direct excitation of these molecules leads to a nonemissive locally excited state (LE) possessing nearly the same dipole moment as the ground state, which subsequently transforms into a more polar emissive state via an intramolecular charge transfer (ICT) process.[19] We had earlier shown that some donor−acceptor-substituted butadienes exhibit the unusual phenomenon of dual emission, with emissions emanating both from the LE and the ICT states.[20]

An increase in the number of alkoxy substituents resulted in a slight red-shift in the emission spectra, and this was accompanied by a significant enhancement in the fluorescence quantum yields and lifetimes (Table 1). The fluorescence spectra of these molecules also undergo a bathochromic shift with increase in solvent polarity, which becomes more pronounced with increase in number of the alkoxy substituents. Figure 1 shows the solvent polarity induced shift in fluorescence spectra of **TBC4**. These effects can be attributed to the presence of each additional alkoxy group causing an enhancement in the electron-donating capabilities of the electron-donating phenyl moiety leading to increased formation of the fluorescent ICT state at the cost of the nonfluorescent LE state.

Photophysical Properties of Thin Films. The fluorescence spectra of the thin films of these molecules were much broader and emission quantum yields were significantly higher compared to that in solution (Table 2) with more than 10-fold enhancement being observed in some cases. As seen from Table 2, the fluorescence spectra of thin films of the monoalkoxy derivatives

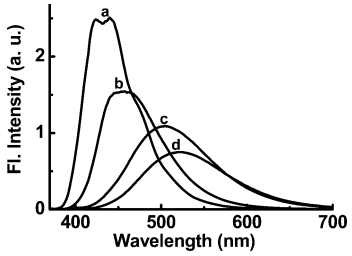

Figure 1. Fluorescence spectra of **TBC4** in solution state (a) *n*-heptane, (b) toluene, (c) THF, and (d) acetonitrile. λ_{ex} = 360 nm.

TABLE 2: Fluorescence Quantum Yields (Φ_f) and CIE Chromaticity Coordinates (1931) of Alkoxy Diphenyl Butadienes in the Solid State

compound	ems. λ_{max} (nm)	Φ_f	fwhm (cm^{-1})	CIE chromaticity coordinates (1931) (x, y)	$\Delta\lambda_{max}$ (nm)[a]
MBC1	505	0.56	5243	0.1688, 0.2897	70
MBC4	495	0.47	4660	0.1462, 0.2037	60
MBC8	463	0.17	4386	0.1613, 0.2711	28
MBC12	450	0.20	4180	0.1691, 0.2611	15
DBC8	543	0.16	2646	0.4238, 0.5900	108
DBC12	543	0.20	2789	0.4129, 0.5728	103
TBC1	500	0.61	3361	0.2777, 0.5661	50
TBC4	498	0.68	3111	0.2460, 0.5901	42
TBC12	497	0.56	3568	0.2713, 0.5562	46

[a] $\Delta\lambda_{max}$ is the difference in the fluorescence maxima between the solid state and the solution emission spectra in toluene.

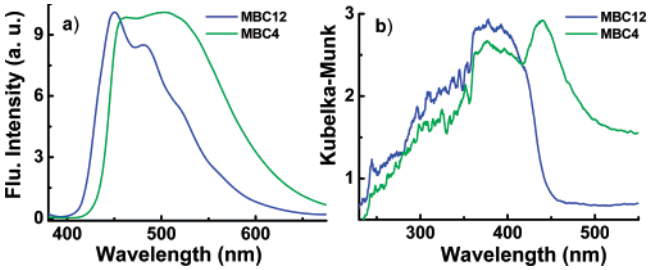

Figure 2. Normalized solid-state (a) fluorescence and (b) reflectance absorption spectra of **MBC12** and **MBC4**.

undergo a blue-shift with increase in length of the alkoxy substituent, whereas those of the di- and tri-alkoxy derivatives are relatively insensitive to the length of the alkoxy substituents.

The solid-state fluorescence and reflectance spectra of the monoalkoxy derivatives reported earlier[12a] are reproduced here for ease of discussion (Figure 2). The fluorescence spectra of the derivatives possessing shorter alkoxy groups (**MBC1**, **MBC4**) were significantly broader and red-shifted compared to that of the derivatives possessing longer alkoxy chains (**MBC8**, **MBC12**). In the reflectance spectra, a new long wavelength peak centered on 447 nm, whose relative intensity increased with decreasing length of the alkyl chain, was also observed. The red-shift observed in the solid state is clearly different from the polarity induced changes observed in solutions. In solution, the red-shift observed on increasing solvent polarity is clearly independent of the length of the alkoxy substituent (Table 1), whereas in the case of the monoalkoxy derivatives, the absorption and emission spectra in the solid state have a significant dependence on the alkoxy chain length. Moreover, in solution, the absorption spectra are not affected by increase in solvent polarity. In the solid state, the derivatives, which show long wavelength fluorescence, clearly show an additional red-shifted peak in the reflectance spectrum indicating the presence of one more ground state absorbing species.

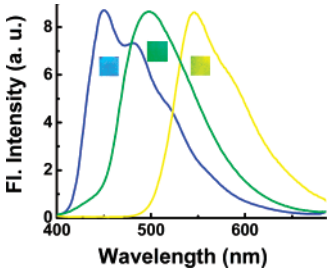

Figure 3. Normalized fluorescence spectra of thin films of **MBC12** (blue spectrum), **DBC12** (yellow spectrum), and **TBC12** (green spectrum). $\lambda_{ex} = 360$ nm. The corresponding fluorescence as visualized on excitation with a 365 nm UV light is also shown.

The normalized fluorescence spectra of thin films of **MBC12**, **DBC12**, and **TBC12** are shown in Figure 3. The red-shift with increasing number of alkoxy substituents is much larger, with the difference in the emission maxima of **DBC12** and **MBC12** being 93 nm. In solution, the corresponding change was 5 nm in toluene and 22 nm in acetonitrile. Moreover, unlike the systematic increase in red-shift with increasing number of alkoxy groups seen in solution (Table 1), the order of red-shift in thin films was **DBC12** > **TBC12** > **MBC12** (Figure 3, Table 2). These results clearly indicate that factors other than purely electronic effects at the molecular level are involved in defining the solid-state fluorescence properties of these materials and suggest that variations in the molecular packing can play a major role in deciding their solid-state fluorescence behavior.

In bulk materials, intermolecular interactions can lead to the formation of aggregates, which can significantly alter the photophysical and photochemical properties of the molecules, resulting in large changes in their spectral characteristics and luminescence efficiency.[7a,21] Two possible explanations can be provided for the large red-shift of the emission maxima and significant enhancement in fluorescence quantum yields of these materials in the solid state compared to that in solution. First, the observed results may be attributed to aggregate formation and exciton coupling. Alternatively, the red-shift in the absorption and emission spectra may be attributed to planarization of the molecule.

To elucidate whether the changes observed in the present system were due to molecular aggregation or were due to planarization, we have prepared solid mixtures in which the diphenylbutadiene derivatives were diluted by an inert material, namely, KBr. If the changes occurring in the solid state were due to planarization, no significant effect on the absorption and emission properties of these compounds would be expected with change in concentration, whereas if the effects were due to formation of aggregates, then under sufficiently dilute conditions it would be possible to generate the monomer form in the solid state. Several solid mixtures containing varying ratios of **DBC12** and KBr were prepared by adding different proportions of **DBC12** dissolved in dichloromethane to KBr in a flask containing excess dichloromethane and by removing the solvent by evaporation under vacuum with vigorous stirring. The emission, excitation, and reflectance absorption spectra of the pure form and a diluted mixture (0.002 mol % of **DBC12** in KBr) is shown in Figure 4. Pure **DBC12** exhibited fluorescence in the long wavelength region with a maximum centered on 545 nm. On dilution of **DBC12** with KBr, along with this long wavelength band, a more narrow emission band with an emission maximum centered on 448 nm, close to the molecular fluorescence measured in toluene, was also observed. This concentration dependent change of the fluorescence maxima of **DBC12** in KBr strongly indicates that dilution by KBr resulted in conversion of the aggregated species observed in pure sample to that of a mixture of monomer and aggregate. The breakup of the aggregates into the monomer species on dilution with KBr was also indicated by a blue-shift in the fluorescence excitation as well as by the reflectance spectra of thin films of **DBC12** (Figure 4b and Figure 4c). The excitation spectra clearly showed the presence of a broad band with a maximum centered at 470 nm. On dilution of **DBC12** with KBr, the excitation maximum shifted to about 388 nm. Similarly, the broad reflectance band observed in pure materials was replaced by a narrower blue-shifted band when it was diluted with KBr. NMR and IR analyses of the compounds recovered from the solid mixtures by solvent extraction confirmed the absence of any chemical transformations because of mixing with KBr.

The breakup of the aggregate could also be investigated by studying the effect of temperature on the spectral properties of thin films of the di- and tri-alkoxy butadiene derivatives. With increasing temperature, a decrease in fluorescence intensity accompanied by a gradual blue-shift and narrowing of the fluorescence band was observed (Figure 5a) (**DBC12**). At 105 °C, which is well below its melting temperature, the fluorescence maximum was centered at about 475 nm, which is between that observed for the monomer of **DBC12** in toluene and acetonitrile solutions. Increase in temperature can lead to a reduction in the strength of the noncovalent intermolecular interactions leading to a breakup of the aggregates into their molecular units. The temperature-induced breakup of the aggregates into the monomeric species was further confirmed by studying the absorption spectra of thin films of **DBC12**. With increase in temperature, the absorption spectra indicated a decrease in intensity in the long wavelength (450−550 nm) region and an increase in intensity of the absorption band centered at 365 nm (Figure 5b). The 365 nm band coincides with the absorption maximum of the monomer species in solution. These effects were fully reversible on cooling. A cross over point at about 435 nm is indicative of a temperature-dependent equilibrium between the monomer and aggregated

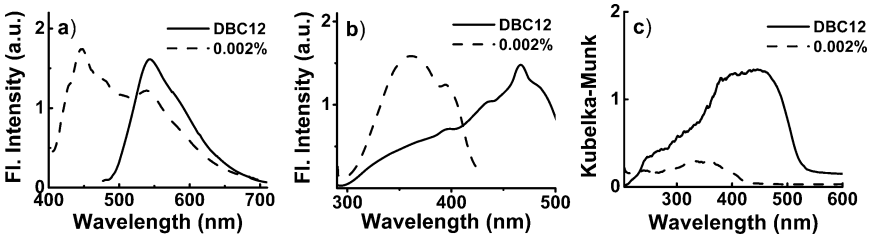

Figure 4. Fluorescence, excitation, and reflectance spectra of pure effect of **DBC12** in pure films and films formed by dilution with KBr on the solid-state (a) fluorescence spectra of (—) pure solid ($\lambda_{ex} = 380$ nm) and (− − −) KBr doped film ($\lambda_{ex} = 450$ nm), (b) excitation spectra of (—) pure solid ($\lambda_{em} = 540$ nm) and (− − −) KBr doped film ($\lambda_{em} = 475$ nm); (c) reflectance absorption spectra of (—) pure solid and (− − −) KBr doped film. Mol% of **DBC12** is indicated in the corresponding figures.

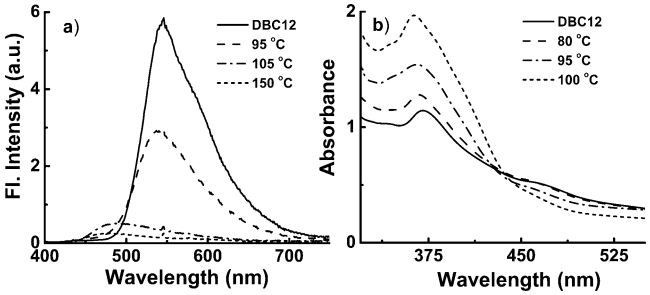

Figure 5. Effect of temperature on the (a) fluorescence (λ_{ex} = 360 nm); (b) absorbance of thin films of **DBC12**.

TABLE 3: Summary of Crystallographic Data for MBC1, MBC4, and MBC8[a]

	MBC1	MBC4	MBC8
empirical formula	$C_{18}H_{15}NO$	$C_{21}H_{21}NO$	$C_{25}H_{29}NO$
molecular weight	261.31	303.39	359.49
crystal system	monoclinic	orthorhombic	monoclinic
space group	*P*2(1)/*c*	*Pna*2(1)	*P*21/*c*
Z	4	4	4
a, Å	6.2803(5)	37.877(4)	8.8931(8)
b, Å	7.1957(6)	6.2281(7)	6.1431(5)
c, Å	30.744(3)	7.0669(8)	37.907(3)
α, deg	90	90	90
β, deg	90.212(1)	90	91.066(6)
γ, deg	90	90	90
V, Å^3	1389.4(2)	1667.1(3)	2070.5(3)
d_{calc}, Mg/cm^3	1.249	1.209	1.153
μ, mm^{-1}	0.077	0.074	0.069
total reflections	8271	9824	17785
unique reflections	3135	2104	4072
R_{int}	0.0230	0.0372	0.078
final *R* indices *R*1, *wR*2	0.0513, 0.1686	0.0446, 0.1276	0.0563, 0.1050
R indices (all data) *R*1, *wR*2	0.0776, 0.2107	0.0602, 0.1553	0.1320, 0.1305

[a] Cambridge crystal data center (CCDC 222238).

species in the thin films. Similar effects were observed for the effect of temperature on the emission and absorption spectra of **TBC12**.[14]

These results clearly indicate that the formation of red-shifted band in the emission and absorption spectra is due to the formation of aggregates and is not merely due to planarization. Moreover, if the effects were only due to planarization, variation in the length of the alkoxy substituents would not be expected to give rise to the large changes in absorption and emission spectra observed in the solid state of the monoalkoxy substituted derivatives. In the case of **MBC8** and **MBC12**, which exhibited a monomer-like fluorescence, a small red-shift of 28 and 25 nm, respectively, was observed between the solid and solution state emission maxima. For these molecules, where aggregation is not observed in the solid state, the small red-shift observed may be attributed to planarization and rigidization of the molecules in the solid state, and a similar contribution could be expected for the other derivatives.[11a]

Crystal Structures. Single crystals of the monoalkoxy substituted derivatives **MBC1**, **MBC4**, and **MBC8** could be grown at room temperature by using solvent mixtures of ethyl acetate and hexane. Their crystal data are summarized in Table 3.

MBC1 has four molecules per unit cell (Figure 6) with the molecules arranged into two nonequivalent stacks and with their dipoles pointing in opposite directions in a herringbone fashion.[22] A part of the X-ray structure of **MBC1** containing four monomer molecules is shown in Figure 7a (see Supporting Information for extended assembly), and this figure can be used to explain all the major intermolecular interactions in the system. From this figure, three major alignments of the molecules can be identified, namely, (1) AB, (2) AA′, and (3) AB′, and these are separately shown in Figure 7b, c, and d, respectively. The B notation is used when the dipole direction (i.e., from acceptor CN to the donor OMe) of the molecules is antiparallel to that of the adjacent A molecule. A′ and B′ designate molecules which are stacked parallel and are slipped along the short axis relative to A and B, respectively.

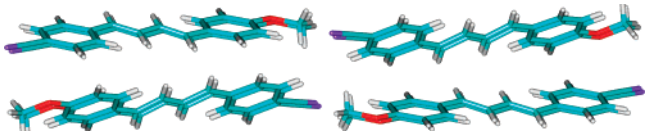

Figure 6. Crystal structure of **MBC1** showing a unit cell.

All the three arrangements of the dimer units presented here show the weak aromatic C−H···π interactions with typical C−H···π distance of around 3.0 Å. Furthermore, aromatic C−H···O in AA′ (2.874 Å) and aliphatic C−H···π interactions (3.083 Å) in AB are also well evident. The shortest C···C distance between two phenyl rings was found to be 3.538 Å, suggesting the possibility of π···π interaction in the system. However, because of the angular arrangement of AB and AB′ dimers, the π···π interaction is expected to be weaker compared to what it would be for a cofacial arrangement of the monomer units. Similarly, π···π stacking interactions between the molecules within each stack, that is, AA′ and BB′, are minimal, since they are slipped along their short axis with respect to each other.

The structure of **MBC4** is very similar to **MBC1** as it shows AB, AA′, and AB′ type dimer units with aromatic C−H···π, aromatic C−H···O, aliphatic C−H···π, and π···π interactions (Figure 8). In addition, the C−H bond of the butyloxy group shows a strong aliphatic C−H···N type hydrogen bond interaction in AB′ (2.693 Å). In fact, the butyl moiety has to adopt a twisted structure to attain the C−H···N type interaction. Compared to **MBC1**, the A and B units of **MBC4** make a larger angle between their aromatic planes while the aromatic planes of the shifted parallel units A and A′ or B and B′ in **MBC4** are located at a larger distance compared to **MBC1** (cf. Figure 7a and 8a), which can be attributed to the larger size of the twisted butyl moiety in **MBC4**.

Although **MBC1** and **MBC4** have very similar arrangements as well as weak interactions in the dimer units, their bulk arrangements differ considerably. For instance, two layers of **MBC1** are arranged in a linear fashion whereas two layers of **MBC4** adopt an angular "V" shaped arrangement (Figure 9). The linear arrangement in **MBC1** is stabilized by a relatively strong aliphatic C−H···N (2.728 Å) interaction when compared to a weaker aliphatic C−H···N (3.030 Å) interaction in **MBC4**.

The structure of **MBC8** is significantly different from those of **MBC1** and **MBC4** (cf. Figure 10). The relative alignment of A and B is the most deviated as they are aligned parallel to each other while in both **MBC1** and **MBC4** they are arranged in an angular fashion with respect to each other. Further, in the AB′ unit, the phenyl rings of both A and B′ occupy nearly the same plane. The AB unit is characterized by the presence of both aliphatic C−H···O and aliphatic C−H···π interactions, whereas two strong intermolecular aromatic C−H···O (2.538 Å) interactions are responsible for the planar AB′ alignment. Such C−H···O hydrogen bonding stabilized crystal structures have been reported for a large class of molecules.[23] In the case of AA′, aliphatic C−H···O and aliphatic C−H···π interactions

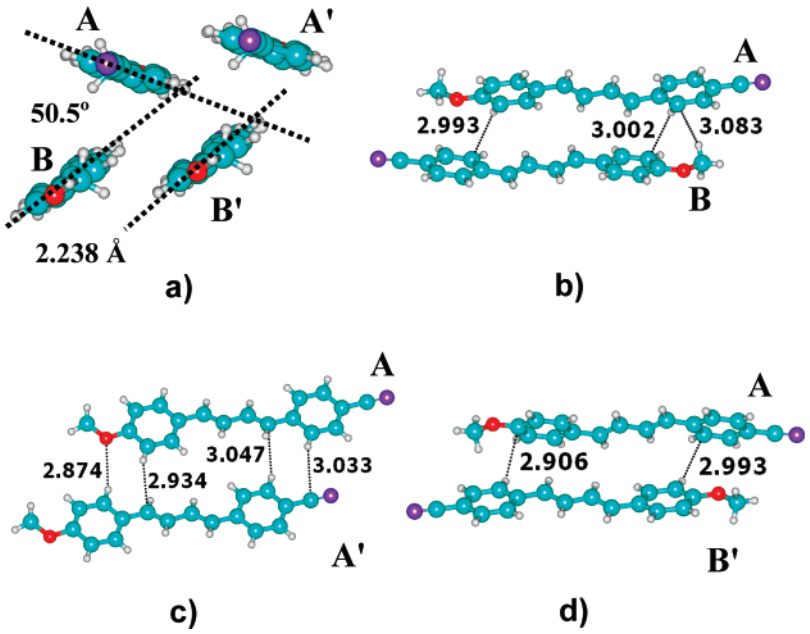

Figure 7. (a) A tetramer unit of **MBC1** taken from the X-ray structure. An axis passing through the CN triple bond (long axis of the molecule) is selected for the view. (b−d) Dimer units showing the AB, AA′, and AB′ interactions. All distances are in angstrom units.

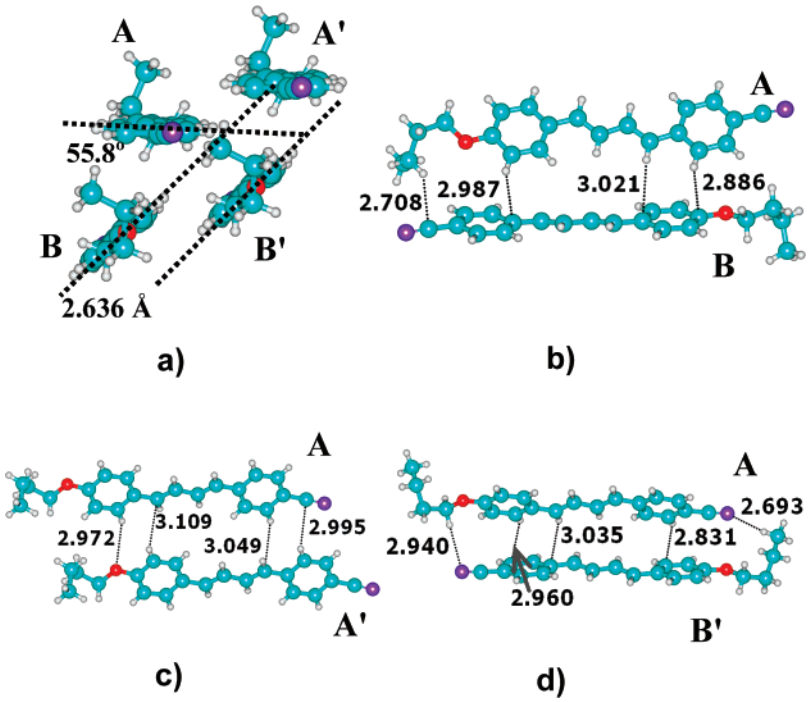

Figure 8. (a) A tetramer unit of **MBC4** taken from the X-ray structure. An axis passing through the CN triple bond (long axis of the molecule) is selected for the view. (b−d) Dimer units showing the AB, AA′, and AB′ interactions. All distances are in angstrom units.

are seen. The aromatic C−H···π interactions are conspicuous by their absence compared to the arrangement of **MBC1** and **MBC4**. Analysis of the weak interactions in the crystal structures suggests that the aromatic C−H···π type interaction is more dominant in **MBC1** and **MBC4** while the molecular packing in **MBC8** is mainly controlled by the aliphatic C−H···O and aliphatic C−H···π type interactions. In **MBC8**, the aromatic π···π interaction is expected to be much weaker compared to **MBC1** and **MBC4** since in the former only the AA′ alignment can contribute to such an interaction while in others all three, namely, AB, AB′, and AA′, can contribute. However, since A and A′ are translated along the short axis relative to each other, the π-overlap between them is also minimal.

Theoretical Calculations. A theoretical study of the X-ray structures corresponding to the dimer and tetramer units of **MBC1**, **MBC4**, and **MBC8** presented in Figures 7, 8, and 10 was conducted in an effort to gain further insight into the variations in the solid-state photophysical properties of these materials. The widely used time-dependent B3LYP/6-31G* level (Becke's three-parameter exchange functional in conjunction with the Lee−Yang−Parr correlation functional and polarized

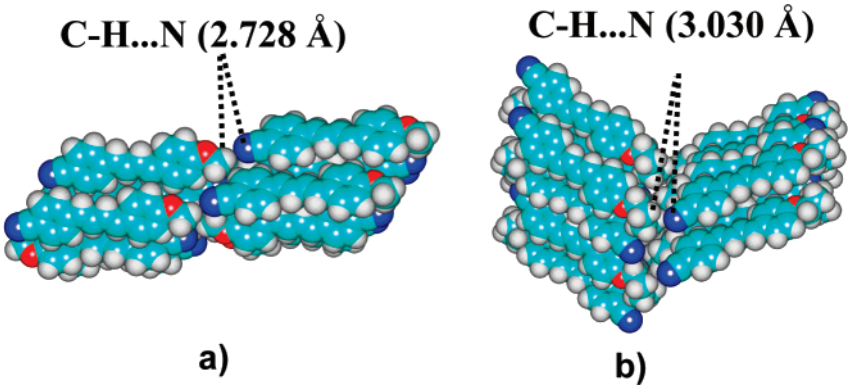

Figure 9. Aliphatic C−H···N interaction in the X-ray structure of (a) **MBC1** and (b) **MBC4**.

spilt-valence basis set) density functional theory method was utilized for this purpose.[24−26] The calculated dipole moment values are depicted in Table 4.

As expected, the electron-donating power of alkoxy group increased with increase in the inductive electron-donating ability of the alkyl moiety ($-OC_8H_{17} > -OC_4H_9 > -OCH_3$), with the highest and lowest dipole moment (DM) values being observed for the monomers of **MBC8** and **MBC1**, respectively. Both **MBC1** and **MBC4** showed the same DM trend for their dimer and tetramer units. Interestingly, although the DM of **MBC1** monomer was the lowest, the DM of its tetramer was higher than that of both **MBC4** and **MBC8**. In fact, the DM of the tetramer unit of **MBC8** was nearly zero because of cancellation of individual monomer DM values, since they existed in nearly perfect antiparallel arrangement. The angular AB and AB′ type arrangement is mainly responsible for a net DM value observed for both **MBC1** and **MBC4**.

The calculated absorption wavelengths for the monomer systems of **MBC1**, **MBC4**, and **MBC8** are 374, 377, and 377 nm, respectively, which are in close agreement with the corresponding experimental values. Further, in all these systems, the electronic transition occurred from a highest occupied molecular orbital (HOMO) mainly centered on the methoxy substituted phenyl ring (donor) to the cyano substituted phenyl ring (acceptor). As an example, the MO features of **MBC1** are illustrated in Figure 11 along with the calculated absorption spectra. The transition dipole moment of value 4.29 D was observed in **MBC1**, which is located in the same direction (close to the long axis of the molecule) as that of the molecular dipole moment. **MBC4** and **MBC8** systems also showed very similar dipole moment features.

Discussion

Aggregation of molecules in the solid state normally leads to quenching of fluorescence, especially when cofacial arrangements are involved. Consequently, enhancement of fluorescence in the solid state has normally been achieved by prevention of aggregation with the help of bulky substituents. In the present study, the solid-state luminescence properties of the donor−acceptor-substituted diphenylbutadiene derivatives are characterized by large red-shifts and enhancement in emission yields compared to that observed in solution. Our experimental studies on the dependence on the absorption and emission spectra on dilution with an inert material such as KBr and on temperature have clearly shown that these effects arise because of aggregation of the molecules in the solid state.

Interaction between the chromophores in their ground state has been explained by Kasha et al. in terms of exciton coupling

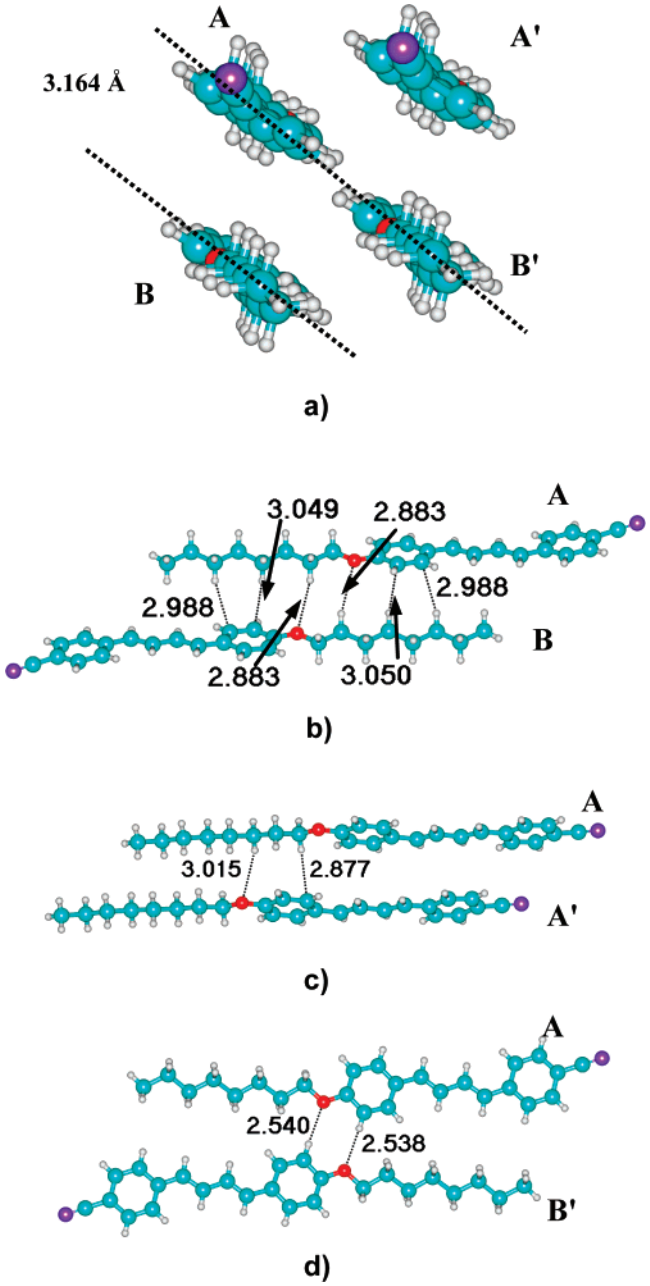

Figure 10. (a) A tetramer unit of **MBC8** taken from the X-ray structure. An axis passing through the CN triple bond (long axis of the molecule) is selected for the view. (b−d) Dimer units showing the AB, AA′, and AB′ interactions. All distances are in angstrom units.

TABLE 4

	dipole moment and transition dipole moment (in debye)		
	MBC1	**MBC4**	**MBC8**
monomer	7.912 (4.29)	8.195 (4.44)	8.522 (4.53)
AB dimer	0.959 (5.60)	0.762 (5.79)	0.008 (6.45)
AA′ dimer	15.137 (5.51)	15.666 (5.75)	16.239 (5.76)
AB′ dimer	0.958 (5.60)	1.219 (5.61)	0.017 (6.52)

theory, in which the excited state of aggregates splits into two energy levels (Davydov splitting).[27] The transition to the upper state is allowed in the case of molecules with cofacial arrangements (H-aggregates), and this is characterized by a hypsochromically shifted absorption band compared to that of the monomer, whereas transition to the lower state is allowed for aggregates arranged in a slipped stack or a head-to-tail fashion (J-aggregates) resulting in a bathochromically shifted absorption band compared to the isolated monomer.

The crystal structure of molecules is usually an extension of the unit structure of aggregates formed in heterogeneous media.[21e] In the present study, thin films of **MBC1** and **MBC4** showed green fluorescence, whereas films of **MBC8** showed blue fluorescence. The fluorescence emission of the films matched closely with that of the corresponding single crystals, indicating that the molecular packing responsible for the luminescent properties was the same in both cases.

The crystal packing of **MBC1**, **MBC4**, and **MBC8** shows that the molecules are stacked in a cofacial manner with the dipole moments of the neighboring stacks pointing in opposite directions. Within each stack, however, the molecules are translated (slipped) along the short axis minimizing the π-overlap between them. The crystal packing of **MBC1** (Figure 7) and **MBC4** (Figure 8) indicates that the electronic interaction is maximum between the molecules of alternate stacks for the AB, AB′ couples which are arranged in a side on manner with respect to each other. In both cases, the dipoles are packed in an antiparallel manner.[28] The red-shifted emission and absorption band centered at 500 and 440 nm, respectively, in the spectra of **MBC1** and **MBC4** confirm that the transition does indeed occur to the lower state.

The molecular packing in the single crystal of **MBC8**, which unlike **MBC1** and **MBC4** exhibited blue fluorescence, was very different. As in the other cases, the molecules are stacked into two nonequivalent stacks with their dipoles pointing in the opposite directions. The molecules which are closest enough to electronically interact with each other are the AB, AB′ couples (Figure 10). From the crystal structure, it becomes evident that in these arrangements the overlap between the diphenylbutadiene chromophore part of these couples is minimal because of the interdigitated arrangement. Instead, the main overlap occurs between the butadiene chromophore of one molecule and the insulating oligomethylene chain of the neighboring molecule. As a result of these factors, electronic interaction between the two molecules is minimized and excitonic coupling does not occur. This is indicated by single molecule like blue fluorescence of **MBC8** and the absence of the long wavelength absorption peak in the reflectance spectrum of its thin film.[12a]

A thin film of **MBC8** obtained by cooling its melt exhibits green fluorescence (λ_{max} = 485 nm) attributable to that of the red-shifted aggregate emission. This form slowly returns to the stable blue fluorescent form (λ_{max} = 463 nm) over a period of 6 h at room temperature. Powder X-ray diffraction (XRD) patterns of the two forms indicated the molecular packing in these two systems to be significantly different. Formation of the metastable state was explained earlier to be due to breaking of the C−H···O hydrogen bonds between molecular pairs and the formation of a layered molecular arrangement.[12a] However, the present study, which shows that in **MBC1** and **MBC4** the aggregation leading to the red-shifted fluorescence occurs through edge-to-face interaction between molecules of adjacent stacks, strongly suggests that the metastable form of **MBC8** exhibiting aggregate fluorescence could have a similar structure. Thus, on heating, the weak AB interactions could break followed by translation of the molecules along the long axis and twist of the aromatic group resulting in an arrangement in which the aromatic units lie close to each other stabilized by edge-to-face interactions as observed in **MBC1** and **MBC4** to give rise to the metastable green fluorescent state on rapid cooling. The proposed changes in the alignment are schematically represented

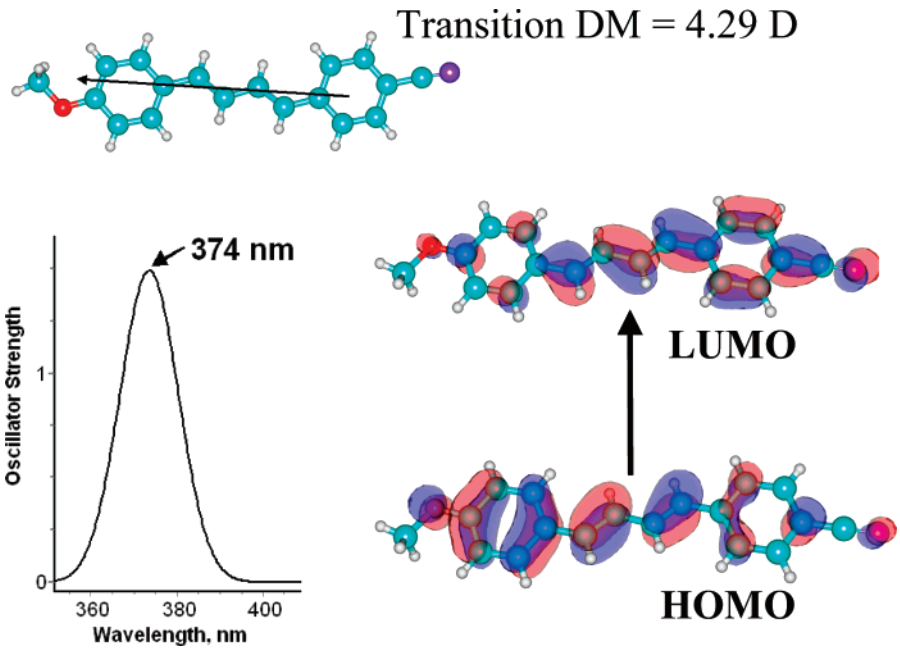

Figure 11. Calculated absorption spectra of **MBC1** monomer. Also shown is the transition dipole moment vector and the HOMO to LUMO electron transition corresponding to the absorption peak.

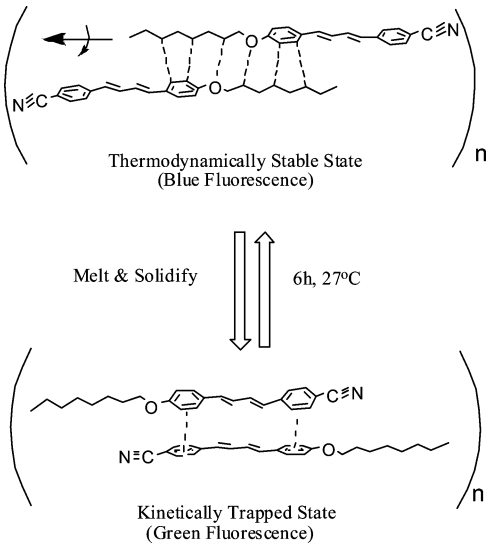

Figure 12. Schematic representation of change in the molecular arrangement within the thermodynamically stable and kinetically trapped forms of **MBC8**.

in Figure 12. This could then slowly evolve over a period of time into the thermodynamically stable arrangement in which stacks are stabilized by C−H···O hydrogen bonds.

Conclusions

Elucidating the molecular basis of the luminescence behavior of bulk materials is of significant importance from the point of view of designing highly luminescent materials for applications in a variety of optoelectronic devices. The alkoxy-cyano substituted diphenylbutadienes described in the present study exhibit significant differences in their fluorescence behavior in the solid state compared to that in solution. We have shown that for this class of molecules the differences are caused predominantly by the formation of highly luminescent aggregates in the solid state and that the formation of such aggregates was strongly dependent on the nature of the alkyl substituents. In the monoalkoxy derivatives, the luminescence of the derivatives possessing shorter alkyl substituents (**MBC1** and **MBC4**) is predominated by the red-shifted aggregate luminescence, whereas the derivatives with longer alkyl substituents show predominantly monomer type fluorescence. Analysis of the molecular packing in the single crystals of the mono-alkoxy substituted derivatives indicates that the dimer aggregate made up of molecules packed edge-to-face with their dipoles stacked in an antiparallel manner are responsible for the red-shifted aggregate emission in **MBC1** and **MBC4**. In the case of the **MBC8**, the presence of the longer alkyl substituent leads to an interdigitated alignment, which prevents the formation of the luminescent dimer. In the derivatives containing more than one alkoxy substituent, such an interdigitated arrangement would be prevented because of steric reasons, as indicated by the absence of the effect of alkoxy chain length variation in the di- and tri-alkoxy substituted derivatives.

Acknowledgment. The research grants from Department of Science and Technology (DST), India, Indo-Japanese Scientific Collaborative Project (IJCSP), and Council of Scientific and Industrial Research Task Force Program (CMM 010) are gratefully acknowledged. We thank Ms. Midori Goto, AIST, Tsukuba, Japan, for X-ray crystallographic analysis. This is contribution no. PPD-239 from RRLT-PPD. R.D., N.S.S.K., and S.A. thank CSIR, Government of India, for research fellowships.

Supporting Information Available: Crystallographic CIF files, details of synthesis, and analytical and spectral characterization data of compounds. The solid-state fluorescence spectra of di- and tri-alkoxy series, effect of temperature on the absorption and fluorescence spectra of **TBC12**, and extended crystal packing of **MBC1**, **MBC4**, **and MBC8** are also provided. This material is available free of charge via the Internet at http://pubs.acs.org.

References and Notes

(1) (a) Hoeben, F. J. M.; Jonkheijm, P.; Meijer, E. W.; Schenning, A. P. H. J. *Chem. Rev.* **2005**, *105*, 1491. (b) Bendikov, M.; Wudl, F.; Perepichka, D. F. *Chem. Rev.* **2004**, *104*, 4891. (c) Hide, F.; Diaz-Garcia, M. A.; Schwartz, B. J.; Heeger, A. J. *Acc. Chem. Res.* **1997**, *30*, 430. (d) Bunz, U. H. F. *Chem. Rev.* **2000**, *100*, 1605. (e) Tour, J. M. *Chem. Rev.* **1996**, *96*, 537. (f) Meng, H.; Sun, F.; Goldfinger, M. B.; Gao, F.; Londono, D. J.; Marshal, W. J.; Blackman, G. S.; Dobbs, K. D.; Keys, D. E. *J. Am. Chem. Soc.* **2006**, *128*, 9304. (g) Forrest, S. R. *Nature* **2004**, *428*, 911. (h) Brédas, J.-L.; Beljonne, D.; Coropceanu, V.; Cornil, J. *Chem. Rev.* **2004**, *104*, 4971.

(2) (a) Burroughes, J. H.; Bradley, D. D. C.; Brown, A. R.; Marks, R. N.; Mackay, K.; Friend, R. H.; Holmes, P. L.; Holmes, A. B. *Nature* **1990**, *347*, 539. (b) Kraft, A.; Reichert, A. *Tetrahedron* **1999**, *55*, 3923. (c) In *Organic Light Emitting Devices: Synthesis, Properties and Applications*; Müllen, K., Scherf, U., Eds.; Wiley-VCH: Weinheim, Germany, 2006. (d) Yamaguchi, Y.; Ochi, T.; Miyamura, S.; Tanaka, T.; Kobayashi, S.; Wakamiya, T.; Matsubara, Y.; Yoshida, Z.-i. *J. Am. Chem. Soc.* **2006**, *128*, 4504. (e) Armaroli, N.; Accorsi, G.; Holler, M.; Moudam, O.; Nierengarten, J.-F.; Zhou, Z.; Wegh, R. T.; Welter, R. *Adv. Mater.* **2006**, *18*, 1313.

(3) (a) O'Neill, M.; Kelly, S. M. *Adv. Mater.* **2003**, *15*, 1135. (b) Shirota, Y. *J. Mater. Chem.* **2005**, *15*, 75. (c) Strohriegl, P.; Grazulevicius, J. V. *Adv. Mater.* **2002**, *14*, 1439.

(4) (a) Dimitrakopoulos, C. D.; Malenfant, P. R. L. *Adv. Mater.* **2002**, *14*, 99. (b) Garnier, F.; Hajlaoui, R.; Yassar, A.; Srivastava, P. *Science* **1994**, *265*, 1684. (c) Li, X.-C.; Sirringhaus, H.; Garnier, F.; Holmes, A. B.; Moratti, S. C.; Feeder, N.; Clegg, W.; Teat, S. J.; Friend, R. H. *J. Am. Chem. Soc.* **1998**, *120*, 2206. (d) Kelly, S. M.; O'Neill, M. In *Handbook of Advanced Electronic and Photonic Materials*; Nalwa, H. S., Ed.; Academic Press: San Diego, CA, 2000; Vol. 1, Chapter 1.

(5) (a) Hudson, A. J.; Weaver, M. S. In *Functional Organic and Polymeric Materials*; Richardson, T. H., Ed.; John Wiley & Sons: New York, 2000. (b) Kaneko, M. In *Handbook of Organic Molecules and Polymers*; Nalwa, H. S., Ed.; Wiley: New York, 1997.

(6) (a) Friend, R. H.; Gymer, R. W.; Holmes, A. B.; Burroughes, J. H.; Marks, R. N.; Taliani, C.; Bradley, D. D. C.; Santos, D. A. D.; Brédas, J. L.; Logdlund, M.; Salaneck, W. R. *Nature* **1999**, *397*, 121. (b) Lewis, F. D.; Yang, J. S. *J. Phys. Chem. B* **1997**, *101*, 1775. (c) Wilson, J. N.; Smith, M. D.; Enkelmannc, V.; Bunz, U. H. F. *Chem. Commun.* **2004**, 1700. (d) Jayanty, S.; Radhakrishnan, T. P. *Chem.—Eur. J.* **2004**, *10*, 2661.

(7) (a) Cornil, J.; Beljonne, D.; Calbert, J.-P.; Brédas, J.-L. *Adv. Mater.* **2001**, *13*, 1053. (b) Datta, A.; Pati, S. K. *Chem. Soc. Rev.* **2006**, *35*, 1305. (c) Pope, M.; Swenberg, C. E. C. E. *Electronic Processes in Organic Crystals and Polymers*; Oxford University Press: New York, 1999. (d) Sun, H.; Zhao, Z.; Spano, F. C.; Beljonne, D.; Cornil, J.; Shuai, Z.; Brédas, J.-L. *Adv. Mater.* **2003**, *15*, 818. (e) Dreuw, A.; Plötner, J.; Lorenz, L.; Wachtveitl, J.; Djanhan, J. E.; Brüning, J.; Metz, T.; Bolte, M.; Schmidt, M. U., *Angew. Chem., Int. Ed.* **2005**, *44*, 7783. (f) Langhals, H.; Potrawa, T.; Nöth, H.; Linti, G. *Angew. Chem., Int. Ed. Engl.* **1989**, *28*, 478. (g) Datta, A.; Terenziani, F.; Painelli, A. *ChemPhysChem* **2006**, *7*, 2168.

(8) (a) Kim, J.; Swager, T. M. *Nature*, **2001**, *411*, 1030. (b) Jenekhe, S. A.; Osaheni, J. A. *Science*, **1994**, *265*, 765. (c) Xie, Z.; Yang, B.; Li, F.; Cheng, G.; Liu, L.; Yang, G.; Xu, H.; Ye, L.; Hanif, M.; Liu, S.; Ma, D.; Ma, Y. *J. Am. Chem. Soc.* **2005**, *127*, 14152.

(9) (a) Curtis, M. D.; Cao, J.; Kampf, J. W. *J. Am. Chem. Soc.* **2004**, *126*, 4318. (b) Mutai, T.; Satou, H.; Araki, K. *Nat. Mater.* **2005**, *4*, 685. (c) Ooyama, Y.; Okamoto, T.; Yamaguchi, T.; Suzuki, T.; Hayashi, A.; Yoshida, K. *Chem.—Eur. J.* **2006**, *12*, 7827. (d) Papaefstathiou, G. S.; Zhong, Z.; Geng, L.; MacGillivray, L. R. *J. Am. Chem. Soc.* **2004**, *126*, 9158. (e) Mizobe, Y.; Tohnai, N.; Miyata, M.; Hasegawa, Y. *Chem. Commun.* **2005**, 1839. (f) Koren, A. B.; Curtis, M. D.; Kampf, J. W. *Chem. Mater.* **2000**, *12*, 1519. (g) Yang, J.-S.; Yan, J.-L.; Hwang, C.-Y.; Chiou, S.-Y.; Liau, K.-L.; GavinTsai, H.-H.; Lee, G.-H.; Peng, S.-M. *J. Am. Chem. Soc.* **2006**, *128*, 14109. (h) Tong, H.; Dong, Y.; Häußler, M.; Lam, J. W. Y.; Sung, H. H.-Y.; Williams, I. D.; Sun, J.; Tang, B. Z. *Chem. Commun.* **2006**, 1133. (i) Kishimura, A.; Yamashita, T.; Yamaguchi, K.; Aida, T. *Nat. Mater.* **2005**, *4*, 546. (j) Shetty, A. S.; Liu, E. B.; Lachicotte, R. J.; Jenekhe, S. A. *Chem. Mater.* **1999**, *11*, 2292. (k) Ooyama, Y.; Yoshikawa, S.; Watanabe, S.; Yoshida, K. *Org. Biomol. Chem.*, **2006**, *4*, 3406. (l) Mizobe, Y.; Ito, H.; Hisaki, I.; Miyata, M.; Hasegawa, Y.; Tohnai, N. *Chem. Commun.* **2006**, 2126.

(10) (a) Deans, R.; Kim, J.; Machacek, M. R.; Swager, T. M. *J. Am. Chem. Soc.* **2000**, *122*, 8565. (b) An, B.-K.; Kwon, S.-K.; Jung, S.-D.; Park, S. Y. *J. Am. Chem. Soc.* **2002**, *124*, 14410. (c) Luo, J.; Xie, Z.; Lam, J. W. Y.; Cheng, L.; Chen, H.; Qiu, C.; Kwok, H. S.; Zhan, X.; Liu, Y.; Zhu, D.; Tang, B. Z. *Chem. Commun.* **2001**, 1740. (d) Chen, J.; Xu, B.; Ouyang, X.; Tang, B. Z.; Cao, Y. *J. Phys. Chem. A* **2004**, *108*, 7522. (e) Li, Z. H.; Wong, M. S.; Tao, Y.; Lu, J. *Chem.—Eur. J.* **2005**, *11*, 3285.

(11) (a) Da Como, E.; Loi, M. A.; Murgia, M.; Zamboni, R.; Muccini, M. *J. Am. Chem. Soc.* **2006**, *128*, 4277. (b) Würthner, F.; Thalacker, C.; Diele, S.; Tschierske, C. *Chem.—Eur. J.* **2001**, *7*, 2245. (c) Siddiqui, S.; Spano, F. C. *Chem. Phys. Lett.* **1999**, *308*, 99. (d) Frolov, S. V.; Vardeny, Z. V.; Yoshino, K. *Phys. Rev. B* **1998**, *57*, 9141. (e) Jelly, E. E. *Nature* **1936**, *138*, 1009. (f) Möbius, D. *Adv. Mater.* **1995**, *7*, 437. (g) Hannah, K. C.; Armitage, B. A. *Acc. Chem. Res.* **2004**, *37*, 845. (h) Whitten, D. G. *Acc. Chem. Res.* **1993**, *26*, 502. (i) Schenning, A. P. H. J.; Jonkheijm, P.; Peeters, E.; Meijer, E. W. *J. Am. Chem. Soc.* **2001**, *123*, 409.

(12) (a) Davis, R.; Rath, N. P.; Das, S. *Chem. Commun.* **2004**, 74. (b) Abraham, S.; Mallia, V. A.; Ratheesh, K. V.; Tamaoki, N.; Das, S. *J. Am. Chem. Soc.* **2006**, 1*28*, 7692. (c) Davis, R.; Abraham, S.; Rath, N. P.; Das, S. *New J. Chem.* **2004**, *28*, 1368. (d) Davis, R.; Das, S. *J. Fluoresc.* **2005**, *15*, 749. (e) Kumar, N. S. S.; Varghese, S.; Narayan, G.; Das, S. *Angew. Chem., Int. Ed.* **2006**, *45*, 6317.

(13) (a) Davis, R.; Mallia, V. A.; Das, S. *Chem. Mater.* **2003**, *15*, 1057. (b) Braatz, H.; Hecht, S.; Seifert, H.; Helm, S.; Bendig, J.; Rettig, W. *J. Photochem. Photobiol., A* **1999**, *123*, 99. (c) Brettle, R.; Dunmur, D. A.; Hindley, N. J.; Marson, C. M. *J. Chem. Soc., Chem. Commun.* **1992**, 410.

(14) See Supporting Information.

(15) (a) De Mello, J. C.; Wittmann, H. F.; Friend, R. H. *Adv. Mater.* **1997**, *9*, 230. (b) Pålsson, L.-O.; Monkman, A. P. *Adv. Mater.* **2002**, *14*, 757. (c) Shah, B. K.; Neckers, D. C.; Shi, J.; Forsythe, E. W.; Morton, D. *Chem. Mater.* **2006**, *18*, 603.

(16) Cölle, M.; Gmeiner, J.; Milius, W.; Hillebrecht, H.; Brütting, W. *Adv. Funct. Mater.* **2003**, *13*, 108.

(17) (a) Sheldrick, G. M. *SHELXTL*, version 6.12; Bruker-AXS: Madison, WI, 2000. (b) Sheldrick, G. M. *SADABS*: *Program for scaling and correction of area detector data*; University of Göttingen, Germany, 1998.

(18) Bruno, I. J.; Cole, J. C.; Edgington, P. R.; Kessler, M.; Macrae, C. F.; McCabe, P.; Pearson, J.; Taylor, R. *Acta Crystallogr., Sect. B: Struct. Sci.* **2002**, *58*, 389.

(19) (a) Rettig, W. In *Topics of Current Chemistry*; Electron Transfer 1; Mattey, J., Ed.; Vol. 169; Springer: Berlin, 1994; p 253. (b) Demeter, A.; Druzhinin, S.; George, M.; Haselbach, E.; Roulin, J.-L.; Zachariasse, K. A. *Chem. Phys. Lett.* **2000**, *323*, 351.

(20) Davis, R.; Das, S.; George, M. V.; Druzhinin, S.; Zachariasse, K. A. *J. Phys. Chem. A* **2001**, *105*, 4790.

(21) (a) Sheikh-Ali, B. M.; Rapta, M.; Jameson, G. B.; Cui, C.; Weiss, R. G. *J. Phys. Chem.* **1994**, *98*, 10412. (b) Sheikh-Ali, B. M.; Weiss, R. G. *J. Am. Chem. Soc.* **1994**, *116*, 6111. (c) Lewis, F. D.; Yang, J.-S.; Stern, C. L. *J. Am. Chem. Soc.* **1996**, *118*, 2772. (d) Lewis, F. D.; Yang, J.-S.; Stern, C. L. *J. Am. Chem. Soc.* **1996**, *118*, 12029. (e) Vaday, S.; Geiger, H. C.; Cleary, B.; Perlstein, J.; Whitten, D. G. *J. Phys. Chem. B* **1997**, *101*, 321.

(22) (a) Koren, A. B.; Curtis, M. D.; Francis, A. H.; Kampf, J. W. *J. Am. Chem. Soc.* **2003**, *125*, 5040. (b) Gierschner, J.; Ehni, M.; Egelhaaf, H.-J.; Medina, B. M.; Beljonne, D.; Benmansour, H.; Bazan, G. C. *J. Chem. Phys.* **2005**, *123*, 144914. (c) Spano, F. C. *J. Chem. Phys.* **2003**, *118*, 981. (d) Nishio, M. *CrystEngComm* **2004**, *6*, 130.

(23) (a) Desiraju, G. R. *Acc. Chem. Res.* **1996**, *29*, 441. (b) Desiraju, G. R. *Acc. Chem. Res.* **2002**, *35*, 565. (c) Vargas, R.; Garza, J.; Dixon, D. A.; Hay, B. P. *J. Am. Chem. Soc.* **2000**, *122*, 4750. (d) Jeffrey, G. A. *An Introduction to Hydrogen Bonding*; Oxford University Press: Oxford, U.K., 1997.

(24) (a) Becke, A. D. *J. Chem. Phys.* **1993**, *98*, 5648. (b) Lee, C.; Yang, W.; Parr, R. G. *Phys. Rev. B: Condens. Matter* **1988**, *37*, 785.

(25) (a) Stratmann, R. E.; Scuseria, G. E.; Frisch, M. J. *J. Chem. Phys.* **1998**, *109*, 8218. (b) Bauernschmitt, R.; Ahlrichs, R. *Chem. Phys. Lett.* **1996**, *256*, 454. (c) Casida, M. E.; Jamorski, C.; Casida, K. C.; Salahub, D. R. *J. Chem. Phys.* **1998**, *108*, 4439.

(26) Frisch, M. J.; Trucks, G. W.; Schlegel, H. B.; Scuseria, G. E.; Robb, M. A.; Cheeseman, J. R.; Montgomery, J.; Vreven, J. A. T.; Kudin, K. N.; Burant, J. C.; Millam, J. M.; Yengar, S. S.; Tomasi, J.; Barone, V.; Mennucci, B.; Cossi, M.; Scalmani, G.; Rega, N.; Petersson, G. A.; Nakatsuji, H.; Hada, M.; Ehara, M.; Toyota, K.; Fukuda, R.; Hasegawa, J.; Ishida, M.; Nakajima, T.; Honda, Y.; Kitao, O.; Nakai, H.; Klene, M.; Li, X.; Knox, J. E.; Hratchian, H. P.; Cross, J. B.; Bakken, V.; Adamo, C.; Jaramillo, J.; Gomperts, R.; Stratmann, R. E.; Yazyev, O.; Austin, A. J.; Cammi, R.; Pomelli, C.; Ochterski, J. W.; Ayala, P. Y.; Morokuma, K.; Voth, G. A.; Salvador, P.; Dannenberg, J. J.; Zakrzewski, V. G.; Dapprich, S.; Daniels, A. D.; Strain, M. C.; Farkas, O.; Malick, D. K.; Rabuck, A. D.; Raghavachari, K.; Foresman, J. B.; Ortiz, J. V.; Cui, Q.; Baboul, A. G.; Clifford, S.; Cioslowski, J.; Stefanov, B. B.; Liu, G.; Liashenko, A.; Piskorz, P.; Komaromi, I.; Martin, R. L.; Fox, D. J.; Keith, T.; Al-Laham, M. A.; Peng, C. Y.; Nanayakkara, A.; Challacombe, M.; Gill, P. M. W.; Johnson, B.; Chen, W.; Wong, M. W.; Gonzalez, C.; Pople, J. A. *Gaussian 03*, revision C.02; Gaussian, Inc.: Wallingford, CT, 2004.

(27) (a) Kasha, M.; Rawls, H. R.; El-Bayoumi, M. A. *Pure Appl. Chem.* **1965**, *11*, 371. (b) Davydov, A. S. *Theory of Molecular Excitons*; Plenum Press: New York, 1971.

(28) (a) Islam, A.; Cheng, C.-C.; Chi, S.-H.; Lee, S. J.; Hela, P. G.; Chen, I.-C.; Cheng, C.-H. *J. Am. Chem. Soc.* **2005**, *109*, 5509. (b) Würthner, F.; Yao, S.; Debaerdemaeker, T.; Wortmann, R. *J. Am. Chem. Soc.* **2002**, *124*, 9431. (c) Rösch, U.; Yao, S.; Wortmann, R.; Würthner, F. *Angew. Chem., Int. Ed.* **2006**, *45*, 7026.